Rapid uptake of gold ions by sulfonated humic acid-derived phenolic resin composite with high adsorption capacity and selectivity

Kun Hou
Henan Agricultural University
Xinshuai Xu
Nanjing Forestry University
Yong Xiang
Zhengzhou University
Xiangmeng Chen
Henan Agricultural University
Su Shiung Lam
Institute of Tropical Aquaculture and Fisheries (AKUATROP), Universiti Malaysia Terengganu
Shengbo Ge (geshengbo@njfu.edu.cn)
Nanjing Forestry University

Research Article

Keywords: sulfonate, humic acid, adsorption, gold, adsorption-reduction-adsorption

Posted Date: January 24th, 2023

DOI: https://doi.org/10.21203/rs.3.rs-2487329/v1

Additional Declarations: No competing interests reported.

Version of Record: A version of this preprint was published at Advanced Composites and Hybrid Materials on March 31st, 2023. See the published version at https://doi.org/10.1007/s42114-023-00647-y.

Abstract

Adsorption capacity, selectivity and adsorption rate are all important indicators to judge the performance of an adsorbent. At present, most of the studies on gold recovery with adsorbents have weakened the consideration of adsorption efficiency. Therefore, there is a need to develop an adsorbent with fast adsorption rate for gold ions to ensure high adsorption capacity and selectivity. Here, we report two humic acid-derived sulfonated resins (SHAR and NSHAR) using sulfuric acid and sodium sulfite as sulfonating agents respectively, which were prepared by a simple two-step method using water as solvent. They can recover Au(III) quickly and efficiently from mixed metals (Fe(III), Mn( ), Cu( ), Cr(III), Mg( ), Ni( ), Sn( ), Co( ), Pb( ) and Zn( )). Adsorption behavior and mechanism of Au(III) on SHAR and NSHAR were studied. The Freundlich isotherm model and the Pseudo-second-order kinetic model are suitably for the description of Au(III) behavior meaning that the process belongs to multi-molecular chemical adsorption. Furthermore, adsorption thermodynamic study indicates that the adsorption of Au(III) on SHAR and NSHAR is endothermic and spontaneous. Different from conventional adsorbents, Au(III) are reduced to element gold and deposited on the adsorbent. NSHAR takes only 10 min to reach adsorption equilibrium, and the adsorption capacity is up to 927 $mg \cdot g^{-1}$ (SHAR needs 50 min with capacity of 1440 $mg \cdot g^{-1}$). This research provides a new scheme and idea for quickly and efficiently recovering gold.

1. Introduction

As a strategic reserve resource, gold plays an irreplaceable role in many fields, such as electronics, medicine, chemicals, and aerospace[1, 2]. With the development of science and technology, the demand for gold has gradually increased, which has accelerated the depletion of gold resources[3]. Therefore, researchers turned their attention to gold-containing e-waste, which is also known as urban minerals, hoping to recover gold from it to ease the exploitation of natural minerals[4, 5]. Among the many recycling technologies, adsorption is considered to be an excellent way to recover secondary resources due to its low-cost and simple operation[6–10].

Humic acid has an uncertain conformation and chemical structure, and belongs to a mixture of macromolecular organic weak acids[11]. It is mainly divided into natural and artificial, with abundant sources.Natural humic acid is organic matter formed from the remains of animals and plants, while artificial humic acid can be obtained from glucose, eucalyptus leaves, etc. as raw materials[12, 13]. Due to the abundant presence of oxygen-containing functional groups (phenolic hydroxyl, carbonyl, carboxyl, etc.), humic acid exhibits good complexing ability for metal oxides and heavy metals[14, 15]. So it has the potential to adsorb gold ions. Nevertheless, humic acid is easy to swell and dissolve in aqueous solution and difficult to be separated from the solution, which limits its application in the field of adsorption. Modification or cross-linking to other materials are commonly used to improve its shortcomings. For example, starch[16], zero-valent iron particles,[13] natural vanadium and titanium-containing magnetite[17] were used to prepare composite materials with humic acid to recover lead ions, showing excellent adsorption properties. T.S. Anirudhan[18] also innovatively prepared the humic acid-aminated

polyacrylamide/ bentonite composite to adsorb Cu(II), Zn(II) and Co(II) ions, and proved the feasibility for humic acid to recycle metal ions. However, there are few studies on the recovery of gold for humic acid or its derivatives. Gatellier[19], Avramenko[20] and Machesky[21] only studied the humic acid in lignite or sludge and found it often accompanied with gold particles. Therefore, it is proposed that there exists interaction between humic acid and gold ions in natural environment and it has the ability to reduce gold ions. In addition, gold is generally widely distributed in the humus layer, and no enriched large ore deposits appear[22–24], which indicates that gold particles cannot stably exist on humic acid. The detailed adsorption behavior and mechanism have not been studied.

In order to utilize the ability of humic acid to absorb and reduce gold ions, and to improve the disadvantages of it as an adsorbent, in our previous work[25], humic acid-derived resin (HAR) was prepared using humic acid as the functional component and phenolic resin as the matrix structure, without using surfactants and template. The phenolic resin was employed because it has the characteristics of low smoke, non-toxicity and easy preparation. Combining it with humic acid can not only reduce the solubility and swelling of humic acid in aqueous solution, but also increase the specific surface area of the composite material. The adsorbent exhibits progressive adsorption performance for gold ions with an adsorption capacity of up to 920 $mg \cdot g^{-1}$ (removal rate of 92%). A downside of HAR is that it takes too long to reach adsorption equilibrium, which greatly reduces the treatment efficiency in practical applications. This is because gold ions are adsorbed by humic acid due to electrostatic interactions and then reduced to elemental gold by phenolic hydroxyl groups. Elemental gold, as it has no electric charge, will break away from HAR and return to the solution under the action of mechanical vibration.When the gold nanoparticles in solution accumulate to a certain size, they can be deposited on the HAR surface again, which takes a long time.

Based on this, according to the hard and soft acid base principle (HSAB), hard acid and hard alkali can form strong bond through coulomb force interaction, while soft acid and soft base can form strong bonds through covalent bond interaction. In theory, therefore, a strong affinity can be formed between gold and soft sulfur atoms[26]. In this work, $-SO_3^-$ was introduced to prepare irregular sulfonated humic acid-derived resin microspheres. The adsorption kinetics, thermodynamics, adsorption behavior and mechanism of gold ions on the new product were systematically examined. The novel adsorbent was applied in column adsorption experiments to recover gold from the simulated leach liquor of ore and circuit board.

2. Experimental

2.1. Materials

Gold standard liquid (99.8% GSB 04-1715-2004) and multielement mixing standard solution were prepared based on the national standard sample (GSB 04 1715–2004). Humic acid (≥ 90%), $FeCl_3 \cdot 6H_2O$ (99%), $Mn(NO_3)_2$ (50 wt. % in H_2O), $Cu(NO_3)_2 \cdot 3H_2O$ (AR), $CrN_3O_9 \cdot 9H_2O$ (99%), $MgSO_4 \cdot 7H_2O$ (≥ 99%),

$NiCl_2·6H_2O$ (AR), $SnCl_2·2H_2O$ (98%), $CoCl_2·6H_2O$ (AR), $PbCl_2$ (99.5%), $ZnCl_2$ (98%) and $HAuCl_4·xH_2O$ (339.79 $g·mol^{-1}$, Au ≥ 47.5%) were purchased from Aladdin. Resorcinol (≥ 99.5%), formaldehyde (37 ~ 40%), sulfuric acid (95% ~ 98%), sodium sulfite (AR), sodium hydroxide (AR) and ammonium hydroxide (25 ~ 28%) were purchased from Sinopharm Chemical Reagent Co., Ltd. Distilled water was made in laboratory. All the reagents were used without further purification.

2.2. Characterization

The concentrations of the metal ions were determined from the inductively coupled plasma-optical emission spectrometer (ICP-OES, PerkinElmer, USA). Fourier transform infrared spectroscopy (FT-IR) measurements were performed on VERTEX 70v (Bruker, Germany) using KBr pellets. Thermogravimetric analyses (TGA) were performed on SDTQ600 (TA, USA, 10 $K·min^{-1}$). X-ray photoelectron spectroscopic (XPS) measurements were performed using an AXIS Supra instrument (China, Al K as Alpha source). N_2 adsorption-desorption was performed using an Autosorb-IQ MP apparatus (USA). Structure characterization was performed by X-ray diffraction (XRD, Bruker AXS D8, scan range: 5°~80°). The structure and morphology were acquired through transmission electron microscopy (TEM, Tecnai G2 F20, China), scanning electron microscope (SEM, zeiss/auriga-bu, Germany) and energy disperse spectroscopy (SEM-EDS). Batch adsorption tests were carried out in the thermostat oscillator (THZ-82B, China).

2.3. Synthesis of sulfonated humic acid-derived resin

The fabrication process of sulfonated humic acid-derived resin was divided into two steps: preparation of sulfonated humic acid and sulfonated humic acid-derived resin.

Synthesis of sulfonated humic acid: In order to introduce the sulfonate group, we used sulfuric acid and sodium sulfite as sulfonating agents to modify humic acid. Each gram of humic acid was mixed with 3 mL sulfuric acid and heated in a water bath at 60℃for 2 h, and then the miscible liquid was placed in a 140°C oven and heated for 24 hours. After cooling to room temperature, wash the product with plenty of water to neutrality, grind it for later use (named as SHA). Humic acid, water and sodium hydroxide with a mass ratio of 12.5:25:1 were stirred to dissolve at 60℃. Then, the sulfonate sodium sulfite (the mass ratio of humic acid to sodium sulfite was 1:3) was added to the solution and stirred at 90 ℃ for 3 h. Subsequently, the pH was adjusted to 4 by 0.5 $mol·L^{-1}$ hydrochloric acid solution, and the precipitated product obtained was sulfonated humic acid (named as NSHA).

Synthesis of sulfonated humic acid-derived resin

Sulfonated humic acid-derived resin was prepared by a modified method[25]. With SHA, formaldehyde and resorcinol as raw materials, ammonia water as catalyst and water as solvent, the pre-polymer was obtained by magnetic stirring at 30℃ for 24 h in a jacketed beaker. Next, the pre-polymer was transferred into the hydrothermal kettle for 8 h at 80℃. The sulfonated humic acid-derived resin (named as SHAR) was obtained by thoroughly removing the unreacted raw material and catalyst with ethanol and water as

detergents. Similarly, other humic acid-derived resins were prepared by replacing SHA with HA and NSHA, respectively (named as HAR and NSHAR).

2.4. Batch adsorption experiment

The batch adsorption experiment was carried out by shaking 10 mL solution with 0.005 g dry SHAR or NSHAR in a brown glass bottle with a mechanical shaker of 200 rpm for some time at specific temperatures. Then, SHAR and NSHAR were separated from the solution by centrifugation. For accuracy, the concentration of the solution was measured three times and averaged.The adsorbents concluding gold (50 mg·g^{-1}) were obtained (named as Au-SHAR and Au-NSHAR) to carry out a series of characterization to investigate adsorption behavior and mechanism. Meanwhile, batch adsorption experiments were employed to investigate the influence of initial concentration (100–900 mg·L^{-1}), pH (1–7) and adsorption time on the adsorptive property. The adsorption isotherms, adsorption thermodynamics and kinetics of gold ions on SHAR and NSHAR were further explored.

Adsorption percentage (q, %) and adsorption capacity (Q, mg·g^{-1}) were calculated according to Eq. (1) and Eq. (2):

$$q = \frac{C_i - C_e}{C_i} \times 100\%$$

1

$$\mathrm{Q} = \frac{C_i - C_e}{m} \times V$$

2

To study the selectivity between other metal ions and Au(III), we simulated the metal concentration and types in the leaching solution of gold ore and waste electronic circuit board of mobile phones respectively, as shown in Table s7[27]. The concentration of gold ions in the waste electronic circuit board leaching solutions are much higher than that of gold ore leaching solution, which explicitly proves the economic value of recycling gold from waste electronic. The separation coefficient between metal ion A and B ($R_{A/B}$) was calculated according to Eq. (3) and Eq. (4) [28]:

$$\mathrm{K} = \frac{(c_i - c_e) \times V}{c_e \times m} = \frac{Q}{c_e}$$

3

$$R_{A/B} = \frac{K_A}{K_B}$$

4

Adsorption kinetics[29] of Au(III) onto SHAR and NSHAR were analyzed by pseudo-first-order kinetic, pseudo-second-order kinetic and intra-particle diffusion models to fit the experimental data, as expressed in Eq. (4), Eq. (5) and Eq. (6):

$$ln\left(Q-Q_t\right)=lnQ-k_1\times t$$

4

$$\frac{t}{Q_t}=\frac{1}{k_2\times Q^2}+\frac{t}{Q}$$

5

$$Q_t=k_{id}\times t^{\frac{1}{2}}+C$$

6

Where, Q_t (mg·g^{-1}) is the adsorption capacity at time *t*. The value of *C* is related to the boundary thickness and *t* (min) is the operation time. k_1, k_2 and k_{id} are the rate constant of pseudo-first-order kinetic, pseudo-second-order kinetic and intra-particle diffusion models.

Adsorption isotherms of Au(III) onto SHAR and NSHAR were analyzed by Langmuir and Freundlich models, expressed as Eq. (7) and Eq. (8):

$$\frac{c_e}{Q}=\frac{c_e}{Q_m}+\frac{1}{K_L\times Q_m}$$

7

$$lnQ=lnK_F+\frac{1}{n}\times lnc_e$$

8

Where, Q_m (mg·g^{-1}) is the maximum adsorption capacity, K_L and K_F are the constant of the Langmuir and Freundlich model. *R* is the gas constant (8.314 J·mol^{-1}· K^{-1}). Generally, a favorable adsorption tends to *1/n* in the range of 0–1.

2.5. Column adsorption experiment

The dynamic adsorption behavior of Au(III) on sulfonated humic acid resin was studied by column adsorption experiment. The schematic of the experimental device is illustrated in Fig. s2(a). The text solution enters the ion-exchange column from the bottom. Since the size of the adsorbent particles reported in this work was in nanometer, large bed resistance caused by traditional top-down feeding was avoided. According to the optimization results, the wet column loading method was employed to fill the

adsorbent. In a special column adsorption experiment, the penetration curve was drawn with 0.1g adsorbent and 1.5 mL·min^{-1} flow rate.

3. Results And Discussion

3.1. Characterization before and after the sulfonated

Figure 1 illustrates the SEM images of HA and HAR before and after introducing the sulfonic acid group. The sulfonation process caused certain damages to the original morphology of HA. SHA particles are looser and have greater damage to HA than NSHA. This is because the sulfonation process of sulfuric acid has a higher temperature and is more destructive. By comparing the structures of HAR, NSHAR and SHAR, it can be found that they are all small irregularly spherical particles with a size ranging from small to large. In addition, as demonstrated in Fig. 1(a-3), (b-3) and (c-3), all of the derived resin can be expropriated as adsorbents for gold recovery.

The functional groups on SHAR and NSHAR surface mainly included –NH_2 and –NH- stretching vibration (3437 cm^{-1}), C = C or C = O vibration (1609 cm^{-1}), -CH_2 stretching (1474 cm^{-1}) and C-O stretch vibration peak (1377 cm^{-1}), as reflected by FT-IR of HAR, SHAR and NSHAR (shown in Fig. 2(a)) [25, 30]. Importantly, asymmetric and symmetric S = O stretching of sulfonic acid groups were observed at 1205 and 1030 cm^{-1} in SHAR and NSHAR FT-IR spectrum[31]. Meanwhile, S 2p components were observed in both the XPS spectra of SHAR and NSHAR (shown in Fig. 2(b)). And the S 2p atomic percentage of SHAR is 0.24% larger than NSHAR (0.18%), which states that the degree of sulfonation of SHAR is higher than that of NSHAR.

As seen from N_2 adsorption-desorption isotherms (Fig. 2 (c) and (d)), both SHAR and NSHAR pertain to typical Type IV isotherm. The average pore size of SHAR and NSHAR are 3.825 nm and 3.056 nm respectively and the specific surface area are 34.56 $m^2 \cdot g^{-1}$ and 142.6 $m^2 \cdot g^{-1}$ respectively (Table s1), which play an important role in their adsorption performance.

3.2. Adsorption comparison before and after sulfonation

To further inspect the adsorption performance of HAR, SHAR and NSHAR, we exposed the derived resin to $HAuCl_4$ solution at different initial concentrations, pH and contact time (Fig. 3). HAR, SHAR and NSHAR all contain some positively charged amino groups. These groups are in charge of electrostatic interaction with gold ions, and the interaction can be effectively adjusted by the pH of the solution. This is because the charge state of the adsorbent surface and the form of metal ions mightily depends on the pH of the solution[27]. When the pH was greater than 8, there was obvious gold sol's precipitation. Therefore, only the change of adsorption capacity with pH of 1–7 was investigated. When the pH was lower than 8, gold ions mainly appeared in negatively charged complexes of $AuCl_4^-$, $Au(OH)Cl_3^-$ and $Au(OH)2Cl_2^-$[32]. Generally, the lower the pH, the more obvious the protonation of the amino group, the more conducive to

the adsorption of gold ions through electrostatic action. However, the lower the pH, the higher the concentration of Cl^- in the liquid phase, which can form competitive adsorption with gold ions and inhibit the adsorption. Consequently, the result of the combined effect is that SHAR at pH = 3 and NSHAR at pH = 4 has better adsorption performance on gold ions. According to previous reports, pH = 3 was beneficial to the adsorption effect of HAR[25]. Therefore, the optimal pH value of each adsorbent was selected to study the maximum adsorption performance.

As shown in Fig. 3(b), the maximum adsorption capacity of SHAR was 1440 $mg \cdot g^{-1}$ (98%), which was higher than that of NSHAR (927 $mg \cdot g^{-1}$, 92.7%) and HAR (920 $mg \cdot g^{-1}$, 92%), and 4 ~ 20 times higher than commercial activated carbon and ion-exchange resins. This might be because SHAR has a higher degree of sulfonation than NSHAR. According to the soft and hard acid-base theory, sulfonate as a soft base can form strong interaction with gold belonging to the soft acid, so the content of sulfonate has a non-negligible effect on the adsorption. At the same initial concentration, the time required for HAR,SHAR and NSHAR to reach adsorption equilibrium for gold ion solution was compared. Excitingly, SHAR requires 50 min and NSHAR only requires 10 min, which is much shorter than HAR (270 min). Both the adsorption capacity and the equilibrium time are improved and superior to other reported adsorbents as seen in Table 1. In practical applications, a shorter adsorption equilibrium time can not only quickly and efficiently treat the waste liquid but also substantially reduce the cost. Here, NSHAR could reach adsorption equilibrium faster than SHAR because the specific surface area of NSHAR was bigger than SHAR (Table s1). It means that more effective functional groups are exposed in the pores, which can quickly catch gold ions and shorten the reaction time.

Table 1
Comparison of SHAR and NSHAR with other adsorbents for gold recovery

Materials	Equilibrium time (min)	Adsorption capacity ($mg \cdot g^{-1}$)	Reference
UiO-66-TU	90	326	[33]
TP	120	1557	[34]
MFRM	750	179.2	[35]
MoS_2	60	1133	[36]
MNP-G3	240	347	[37]
BTU-PT	360	502	[38]
QAPT gel	300	403	[39]
Modified straw	120	450	[40]
HCSs-M	300	1115	[28]
SHAR	50	1440	This work
NSHAR	10	927	

3.3. Adsorption kinetics and isotherms

The kinetic fitting curves and parameters of Au(III) on SHAR and NSHAR are listed in Fig. 4 and Table s2, respectively. The results show that the pseudo -second-order models of the two adsorbents all have a better fit than the pseudo -first-order models. This indicates that the valence bond force is generated between gold ions and adsorbent by sharing or exchanging electrons, and the adsorption process belongs to chemical adsorption[13]. For the solid-liquid adsorption process, there are three consecutive steps for the adsorption of Au(III) on SHAR and NSHAR: (1) the diffusion of Au(III) to the outer surface of the adsorbent (2) the diffusion of Au(III) in the pores of adsorbent and (3) the adsorption of Au(III) on the inner surface. The third stage is usually ignored due to its rapid progress[41]. The speed-limiting steps can be easily found by fitting the experimental data with intra-particle diffusion model. The method of piecewise linear regression was used to divide the curve into different linear regions[42], which avoids subjective judgment when choosing the start and end points of each region. As shown in Fig. 4(b). The last process indicates that the adsorption has reached equilibrium due to $k_{id3} < 1$. The adsorption of gold ions on the SHAR is divided into two stages, film diffusion and pore diffusion. Furthermore, the rate-controlling step is pore diffusion ($k_{id2} > k_{id1}$), due to the low specific surface area of SHAR and insufficient pore channels[42]. However, in the process of NSHAR capturing gold ions, the adsorption process was only divided into one stage, and there was no obvious boundary between interface diffusion and pore diffusion, which is due to the rich pore structure of NSHAR and the fast adsorption process.

The isotherm fitting curves and parameters of Au(III) on SHAR and NSHAR are listed in Fig. 5(a) and Table s3, respectively. In general, for the isotherms of SHAR and NSHAR, the Freundlich model is more suitable, indicating that the adsorption of Au(III) on SHAR and NSHAR belongs to multilayer adsorption. In addition, the value of 1/n is between 0 and 1, and the n of SHAR is greater than that of NSHAR, which reflects that Au(III) is easy to adhere to the adsorbent, and the interaction between SHAR and Au(III) is stronger than that of NSHAR and Au(III)[27]. This also provides evidence that SHAR has a higher adsorption capacity than NSHAR. Furthermore, the change of Gibbs free energy (ΔG°) and enthalpy (ΔH°) were calculated according to the Van't Hoff equation (listed in the Table s4). The negative ΔG° and positive ΔH° imply a spontaneous and endothermic adsorption process.

3.4. Adsorption mechanism

In the process of adsorption, the color of the adsorption solution had a magical change (yellow-pink-purple-blue-colorless) as time increased, which corresponds to the typical color change during the growth of gold colloidal particles. This phenomenon intuitively indicates that Au( ) was reduced during the adsorption process. The standard reduction potentials of Au( )/Au( ) and Au( )/ Au(0) are 1.4 V and 1.0 V. Therefore, in general, Au( ) is first reduced to Au( ), and then Au( ) is reduced to Au(0) [27]. The XRD diffraction analysis can prove that elemental gold appeared on the adsorbent. As presented in Fig. 6(a), there are sharp peaks at 38.13°, 44.32°, 64.60° and 77.62° corresponding to the (111), (200), (220), (311) crystal plane of elemental gold[40], indicating that the gold ions are indeed reduced during the adsorption

process by SHAR and NSHAR. However, in the XPS survey spectra, not only Au 4f is observed, but also the Cl 2p, which shows that the gold species adsorbed on SHAR and NSHAR is a mixture of gold element and gold compounds containing chlorine. In order to explore the specific forms and percentage of gold species, XPS Au 4f narrow scan of Au-SHAR and Au-NSHAR were analyzed in detail. According to the results of Fig. 6(c) and Table s5, it can be seen that most of the gold species attached to adsorbent are Au(0) (68.6%, 65.7%), a small part are Au( ) (34.3%, 31.4%) and no Au( ). This means that Au( ) was completely reduced. The same conclusion can be drawn from the elemental analysis results of SEM-EDS. According to the weight percentages of gold and chlorine in Fig. 6(d) and (e), the corresponding molar ratio of gold to chlorine can be calculated, which is greater than 0.33 ($AuCl_3$) and 1 (AuCl). Gold nanoparticles are also found in the SEM and TEM images. In conclusion, it is clear that the redox reaction occurs when Au( ) is captured by SHAR and NSHAR.

According to reports, $AuCl_4^-$ can be reduced to Au(0) by the abundant hydroxyl groups in the biosorbent, and the hydroxyl groups are oxidized to carbonyl groups[28, 43–45]. In our previous work, it was also found that when HAR adsorbed Au( ) from acidic aqueous solution, Au( ) was reduced by hydroxyl groups[25]. What is the adsorption mechanism of SHAR and NSHAR when they quickly adsorb gold? Further investigation is required. Therefore, XPS C 1s, O 1s, N 1s and S 2p narrow scans of the adsorbent before and after adsorption were analyzed in detail. Taking SHAR as an example, the peaks of C1s (Fig. s1(a)) appear at 284.27 eV, 284.98 eV, 286.12 eV, 287.46 eV and 290.96 eV, assigned to C = C, C-C/C-H, C-O, C = O and O-C = O, respectively[46]. After adsorption, the percentage of C-O decreases from 32.8–29.3% while C = O increases from 9.8–15.5% (Table s6). The O 1s peaks (Fig. s1(b)) correlated to CO-O, $-SO_3^-$, C = O and C-O appears at 530.87 eV, 531.89 eV, 532.69 eV and 533.42 eV, respectively[47]. Likewise, after adsorption, the percentage of C-O reduced while C = O increased, implying that C-O was oxidized to C = O during the adsorption process. The two peaks of N 1s shift to higher Bes, but the percentage has no significant changes. This indicates that there exist covalent bonds between nitrogen atoms and gold atoms[48] that do not participate in the redox reaction. The S 2p curve shown in Figure s1(d) roughly contains two peaks of sulfonate at ~ 162ev and sulfonate at ~ 168ev. Before adsorption, it mainly exists in the form of sulfonate (90.9%), and after adsorption, it mainly exists in the form of sulfide Au-S (79.5%)[49].This evidence suggests that $-SO_3^-$ is involved in the reaction and forms stable Au-S bonds after adsorption.

In summary, the possible adsorption mechanism of gold ions on SHAR and NSHAR can be proposed: Au( ) is uptaked by SHAR and NSHAR with electrostatic interaction and coordinationi nteracts through nitrogen-containing functional groups, and covalent bond with $-SO_3^-$. Then, Au( ) is reduced to Au( ) and Au(0) by C-O groups. Finally, Au( ) and Au(0) are stabilized on the adsorbent. The introduction of $-SO_3^-$ plays a key role in the adsorption process because Au(0) has no positive charge and could not be stably stored on the adsorbent surface through electrostatic interaction. Therefore, the reduced product gold particles are easily released into the liquid phase. As a result, the adsorption solution showed a color change of gold sol. Thus, the introduction of sulfonic acid groups not only accelerates the recovery rate of Au( ) by SHAR and NSHAR, but also increases their adsorption capacity.

3.5. Recovery of gold and competitive adsorption of Au(III) in other metal ions

Since SHAR and NSHAR has the same adsorption mechanism for gold ions, and the adsorption capacity of SHAR is larger than NSHAR, we took SHAR as a representative to investigate the selectivity of metal ions on sulfonated humic acid-derived resin. The types and concentrations of base metal ions in the adsorption solution simulated the leaching solution of gold ore and waste electronic circuit boards. As shown in Fig. 7, under competing conditions, SHAR shows excellent selectivity to gold ions in the leaching solution. By comparison, it is found that the selectivity to gold ions in the leaching solution of the electronic board is better, which may be because the concentration of gold ions and base metal ions in the leaching solution of ore is generally low, leading to a poor separation effect. However, the recovery rate of gold ions is much higher than that of other metal ions, which basically satisfies the practical application.

In order to directly recover gold on the adsorbent, an incineration process is further employed, during which the gold species are reduced to the metal form as the organic components are oxidized. Since gold is more expensive than base metals, and the preparation cost of sulfonated humic acid-based resin is inexpensive than other artificial resins, it is an economical and good choice to recover gold from SHAR by incineration. Au-SHAR was incinerated at 600℃ to remove organic components and directly recover gold from Au-SHAR (Fig. 7(e)). According to the XRD curve in Fig. 7(f), the burning product belongs to element gold.12

3.5. Column adsorption

As shown in Fig. s2(a), Au(III) solution entered the ion exchange column from below, avoiding bed resistance caused by small adsorbent particles. 0.1 g resin was soaked by water for 4 h, and packed into the column in a wet state. At a temperature of 298 K, the Au(III) solution with a concentration of 100 $mg{\cdot}mL^{-1}$ was pumped into the column through a peristaltic pump, and the flow rate was controlled to 1.5 $mL{\cdot}min^{-1}$. In order to better compare the influence of the introduction of sulfonate on the dynamic adsorption, NSHAR and HAR were selected to draw the penetration curve. Because they have a considerable maximum adsorption capacity, which is more convenient for us to clearly evaluate the effect of adsorption rate on the penetration speed. It can be observed from Fig. s2(b) that HAR reached penetration faster than NSHAR. According to the static adsorption experiment, 0.1 g of HAR and NSHAR can capture 92 mg and 92.7 mg gold, respectively. However, the dynamic adsorption capacities of HAR and NSHAR in the column adsorption experiment are 45 mg and 71 mg. The utilization of the resin increased from 48.9–67%. This is because in continuous experiments, the contact time between Au(III) and the adsorbent is relatively short, while HAR has a slow adsorption rate for Au(III), which leads to insufficient adsorption and low utilization rate. In summary, the introduction of $-SO_3^-$ into humic acid-derived resin to shorten the adsorption equilibrium time can not only improve efficiency but also save costs, which has important value in practical application.

4. Conclusion

Sulfuric acid and sodium sulfite were used as sulfonating agents to successfully introduce -SO_3^- into the humic acid-derived resin. SHAR and NSHAR had a faster adsorption rate and higher adsorption capacity for gold ions than HAR. The adsorption mechanism is regarded to comprise physicochemical interactions between gold ions and groups present on SHAR or NSHAR, typically including (1) electrostatic interaction between protonated amino and Au(III), (2) reduction of Au(III) by C-O groups and (3) immobilization of gold with stable Au-s bond. Through column adsorption experiments, the introduction of sulfonic acid groups not only accelerates the adsorption rate, but increases the utilization efficiency of NSHAR in the dynamic adsorption process. This has great economic value in practical applications. In addition, this research uses simple and economical techniques to selectively extract expensive gold from simulated gold ore and electronic board leaching solution, which can recycle secondary resources and conform with the goal of circular economy.

Declarations

Authors' contribution

Kun Hou and Xiangmeng Chen wrote the main manuscript text, Xinshuai Xu and Yong Xiang prepared all the figures, Su Shiung Lam edited the main manuscript text, Shengbo Ge revised and supported funding. All authors reviewed the manuscript.

Funding

The authors thank the National Natural Science Foundation of China (32201491), China Postdoctoral Science Foundation (2021M690847), Natural Science Foundation of Jiangsu Province (BK20200775), Natural Science Foundation of the Jiangsu Higher Education Institutions of China (21KJB220011), Science and Technology Innovation Program of Hunan Province (2021RC2106), Deputy General Project of Science and Technology of Jiangsu Province (FZ20211507).

Acknowledgements

The authors thank the National Natural Science Foundation of China (32201491), China Postdoctoral Science Foundation (2021M690847), Natural Science Foundation of Jiangsu Province (BK20200775), Natural Science Foundation of the Jiangsu Higher Education Institutions of China (21KJB220011), Science and Technology Innovation Program of Hunan Province (2021RC2106), Deputy General Project of Science and Technology of Jiangsu Province (FZ20211507).

Competing interests The authors declare no competing interests.

References

1. Hu CH, Xu WF, Li H, Zhou SX, Mo XH, Zhang PL, Tang KW (2019) Highly efficient adsorption of Au(III) from water by a novel metal-organic framework constructed with sulfur-containing ligands and Zn(II). Ind Eng Chem Res 58:17972-17979. https://doi.org/10.1021/acs.iecr.9b034332
2. Chakarova K, Strauss I, Mihaylov M, Drenchev N, Hadjiivanov K (2019) Evolution of acid and basic sites in UiO-66 and UiO-66-NH_2 metal-organic frameworks: FTIR study by probe molecules. Microporous Mesoporous Mater 281:110-122. https://doi.org/10.1016/j.micromeso.2019.03.006
3. Lin S, Reddy DHK, Bediako JK, Song MH, Wei W, Kim JA, Yun YS (2017) Effective adsorption of Pd(II), Pt(IV) and Au(III) by Zr(IV)-based metal-organic frameworks from strongly acidic solution. J Mater Chem A 5:13557-13564 https://doi.org/10.1039/C7TA02518A
4. Zhang Y, Wang CH, Qu RJ, Gu QY (2011) A resin with high adsorption selectivity for Au (III): Preparation, characterization and adsorption properties. Chem Eng J 172:713-720. https://doi.org/10.1016/j.cej.2011.06.040
5. Awual MR, Khaleque MA, Ferdows M, Chowdhury AMS, Yaita T (2013) Rapid recognition and recovery of gold(III) with functional ligand immobilized novel mesoporous adsorbent. Microchem J 110:591-598. https://doi.org/10.1016/j.microc.2013.07.010
6. Wu ZB, Zhong H, Yuan XZ, Wang H, Wang LL, Chen XH, Zeng GM, Wu Y (2014) Adsorptive removal of methylene blue by rhamnolipid-functionalized graphene oxide from wastewater. Water Res 67:330-344. https://doi.org/10.1016/j.watres.2014.09.026
7. Guo L et al (2021) Synthesis and characterization of ZnNiCr-layered double hydroxides with high adsorption activities for Cr(VI). Adv Compos Hybrid Mater 4(3):819-829. https://doi.org/10.1007/s42114-021-00260-x
8. Gu HB, Gao C, Zhou XM, Du A, Naik N, Guo ZH (2021) Nanocellulose nanocomposite aerogel towards efficient oil and organic solvent adsorption. Adv Compos Hybrid Mater 4(3):459-468. https://doi.org/10.1007/s42114-021-00289-y
9. Liang Y et al (2022) Guanidinium-based ionic covalent organic frameworks for capture of uranyl tricarbonate. Adv Compos Hybrid Mater 5(1):184-194. https://doi.org/10.1007/s42114-021-00311-3
10. Wu QZ et al (2022) Aminated lignin by ultrasonic method with enhanced arsenic (V) adsorption from polluted water. Adv Compos Hybrid Mater 5(2):1044-1053. https://doi.org/10.1007/s42114-022-00492-5
11. Xing BL, Yuan RF, Zhang CX, Huang GX, Guo H, Chen ZF, Chen LJ, Yi GY, Zhang YD, Yu JL (2017) Facile synthesis of graphene nanosheets from humic acid for supercapacitors. Fuel Process Technol 165:112-122. https://doi.org/10.1016/j.fuproc.2017.05.021l
12. Yang T, Hodson ME (2018) Investigating the potential of synthetic humic-like acid to remove metal ions from contaminated water. Sci Total Environ 635:1036-1046. https://doi.org/10.1016/j.scitotenv.2018.04.176
13. Du Q, Li GX, Zhang SS, Song JP, Zhao Y, Yang F (2020) High-dispersion zero-valent iron particles stabilized by artificial humic acid for lead ion removal. J Hazard Mater 383:121170. https://doi.org/10.1016/j.jhazmat.2019.121170

14. Hankins NP, Lu N, Hilal N (2006) Enhanced removal of heavy metal ions bound to humic acid by polyelectrolyte flocculation. Sep Purif Technol 51:48-56. https://doi.org/10.1016/j.seppur.2005.12.022
15. Zhu YY, Chen MM, Li Q, Yuan C, Wang CY (2017) High-yield humic acid-based hard carbons as promising anode materials for sodium-ion batteries. Carbon 123:727-734. https://doi.org/10.1016/j.carbon.2017.08.030
16. Chen RP, Zhang YL, Shen LF, Wang XY, Chen JQ, Ma AJ, Jiang WM (2015) Lead(II) and methylene blue removal using a fully biodegradable hydrogel based on starch immobilized humic acid. Chem Eng J 268:348-355. https://doi.org/10.1016/j.cej.2015.01.081
17. Lu MM, Zhang YB, Zhou YL, Su ZJ, Liu BB, Li GH, Jiang T (2019) Adsorption-desorption characteristics and mechanisms of Pb(II) on natural vanadium, titanium-bearing magnetite-humic acid magnetic adsorbent. Powder Technol 344:47-958. https://doi.org/10.1016/j.powtec.2018.12.081
18. Anirudhan TS, Suchithra PS (2010) Heavy metals uptake from aqueous solutions and industrial wastewaters by humic acid-immobilized polymer/bentonite composite: Kinetics and equilibrium modeling. Chem Eng J 156:146-156. https://doi.org/10.1016/j.cej.2009.10.011
19. Gatellier JP, Disnar JR (1990) Kinetics and mechanism of the reduction of Au(III) to Au(0) by sedimentary organic materials. Org Geochem 16:631-640. https://doi.org/10.1016/0146-6380(90)90076-C
20. Avramenko VA, Bratskaya SY, Yakushevich AS, Voit AV, Ivanov VV, Ivannikov SI (2012) Humic acids in brown coals from the southern Russian far east: General characteristics and interactions with precious metals. Geochem Int 50:437-446. https://doi.org/10.1134/S0016702912030032
21. Machesky ML, Andrade WO, Rose AW (1992) Interactions of gold (III) chloride and elemental gold with peat-derived humic substances. Chem Geol 102:53-71. https://doi.org/10.1016/0009-2541(92)90146-V
22. Yustiawati et al (2015) Effects of peat fires on the characteristics of humic acid extracted from peat soil in Central Kalimantan. Indonesia Environ Sci Pollut Res 22:2384-2395. https://doi.org/10.1007/s11356-014-2929-1
23. Hough RM, Noble RRP, Reich M (2011) Natural gold nanoparticles. Ore Geol Rev 42(1):55-61. https://doi.org/10.1016/j.oregeorev.2011.07.003
24. Arbuzov SI Rikhvanov LP, Maslov SG (2006) Anomalous gold contents in brown coals and peat in the south-eastern region of the Western-Siberian platform. Int J Coal Geol 68:127-134. https://doi.org/10.1016/j.coal.2006.01.004
25. Chen XM, Yang XC, Xiang Y, Xu L, Liu GJ (2020) Humic acid derived resin: an efficient adsorbent for Au(III) uptake from aqueous acidic solution. J Chem Eng Data 65:1824-1832. https://doi.org/10.1021/acs.jced.9b01085
26. Nath S, Ghosh SK, Kundu S, Praharaj S, Panigrahi S, Pal T (2006) Is gold really softer than silver? HSAB principle revisited. J Nanopart Res 8:111-116. https://doi.org/10.1007/s11051-005-8025-1

27. Yang FC, Yan ZG, Zhao J, Miao ST, Wang D, Yang P (2020) Rapid capture of trace precious metals by amyloid-like protein membrane with high adsorption capacity, selectivity. J Mater Chem A 8:3438-3449. https://doi.org/10.1039/c9ta12124b
28. Wang FC, Zhao JM, Zhu MH, Yu JZ, Hu YS, Liu HZ (2014) Selective adsorption-deposition of gold nanoparticles onto monodispersed hydrothermal carbon spherules: a reduction-deposition coupled mechanism. J Mater Chem A 3:1666-1674. https://doi.org/10.1039/c4ta05597g
29. Wang TR, Wusigale, Kuttappan D, Amalaradjou MA, Luo YG, Luo YC (2021) Polydopamine-coated chitosan hydrogel beads for synthesis and immobilization of silver nanoparticles to simultaneously enhance antimicrobial activity and adsorption kinetics. Adv Compos Hybrid Mater 4(3):696-706. https://doi.org/10.1007/s42114-021-00305-1
30. Ming GT, Duan HD, Meng X, Sun GM, Sun WJ, Liu Y, Lucia L (2016) A novel fabrication of monodisperse melamine-formaldehyde resin microspheres to adsorb lead (II). Chem Eng J 288:745-757. https://doi.org/10.1016/j.cej.2015.12.007
31. Seo DC, Jeon I, Jeong ES, Jho JY (2020) Mechanical properties and chemical durability of nafion/sulfonated graphene oxide/cerium oxide composite membranes for fuel-cell applications. Polymers 12:1375-1386. https://doi.org/10.3390/polym12061375
32. Aydin A, Imamoglu M, Gulfen M (2010) Separation and recovery of gold(III) from base metal ions using melamine–formaldehyde-thiourea chelating resin. J Appl Polym Sci 107:1201-1206. https://doi.org/10.1002/app.27178
33. Wu C, Zhu XY, Wang Z, Yang J, Li YS, Gu JL (2017) Specific recovery and in situ reduction of precious metals from waste to create MOF composites with immobilized nanoclusters. Ind Eng Chem Res 56:13975-13982. https://doi.org/10.1021/acs.iecr.7b02839
34. Li YC, Tian HY, Xiao CS, Ding JX, Chen XS (2014) Efficient recovery of precious metal based on Au-S bond and electrostatic interaction. Green Chem 16:4875-4878. https://doi.org/10.1039/c4gc01375a
35. Li QY, Liu JJ, Sun X, Xu L (2019) Hierarchically porous melamine-formaldehyde resin microspheres for the removal of nanoparticles and simultaneously as the nanoparticle immobilized carrier for catalysis. ACS Sustainable Chem Eng 7:867-876. https://doi.org/10.1021/acssuschemeng.8b04490
36. Feng B, Yao CZ, Chen SY, Luo R, Liu SH, Tong SS (2018) Highly efficient and selective recovery of Au(III) from a complex system by molybdenum disulfide nanoflakes. Chem Eng J 350:692-702. https://doi.org/10.1016/j.cej.2018.05.130
37. Yen CH, Lien HL, Chung JS, Yeh HD (2017) Adsorption of precious metals in water by dendrimer modified magnetic nanoparticles. J Hazard Mater 322:215-222. https://doi.org/10.1016/j.jhazmat.2016.02.029
38. Gurung M, Adhikari BB, Kawakita H, Ohto K, Inoue K, Alam S, (2012) Selective recovery of precious metals from acidic leach liquor of circuit boards of spent mobile phones using chemically modified persimmon tannin gel. Ind Eng Chem Res 51:11901-11913. https://doi.org/10.1021/ie3009023
39. Gurung M, Adhikari BB, Khunathai K, Kawakita H, Ohto K, Harada H, Inoue K (2011) Quaternary amine modified persimmon tannin gel: an efficient adsorbent for the recovery of precious metals

from hydrochloric acid media. Sep Sci Technol 46:2250-2259. https://doi.org/10.1080/01496395.2011.594698

40. Wang JJ, Li J, Wei J (2015) Adsorption characteristics of noble metal ions onto modified straw bearing amine, thiol groups. J Mater Chem A 3:18163-18170. https://doi.org/10.1039/c5ta05371d
41. Anirudhan TS, Suchithra PS, Rijith S (2008) Amine-modified polyacrylamide-bentonite composite for the adsorption of humic acid in aqueous solutions. Colloids Surf A 326:147-156. https://doi.org/10.1016/j.colsurfa.2008.05.022
42. Zhao FP, Repo E, Sillanpaa M, Meng Y, Yin DL, Tang WZ (2015) Green synthesis of magnetic EDTA- and/or DTPA-cross-linked chitosan adsorbents for highly efficient removal of metals. Ind Eng Chem Res 54:1271-1281. https://doi.org/10.1021/ie503874x
43. Pangeni B, Paudyal H, Abe M, Inoue K, Kawakita H, Ohto K, Adhikari BB, Alam S (2012) Selective recovery of gold using some cross-linked polysaccharide gels. Green Chem 14:1917-1927. https://doi.org/10.1039/c2gc35321k
44. Gurung M, Adhikari BB, Kawakita H, Ohto K, Inoue K, Alam S (2011) Recovery of Au(III) by using low cost adsorbent prepared from persimmon tannin extract. Chem Eng J 174:556-563. https://doi.org/10.1016/j.cej.2011.09.039
45. Adhikari CR, Parajuli D, Inoue K, Ohto K, Kawakita H, Harada H (2008) Recovery of precious metals by using chemically modified waste paper. New J Chem 32:1634-1641. https://doi.org/10.1039/b802946f
46. Shen Y, Chen BL (2015) Sulfonated graphene nanosheets as a superb adsorbent for various environmental pollutants in water. Environ Sci Technol 49:7364-7372. https://doi.org/10.1021/acs.est.5b01057
47. Shao DD, Jiang ZQ, Wang XK (2010) SDBS Modified XC-72 carbon for the removal of Pb(II) from aqueous Ssolutions. Plasma Processes Polym 7:552-560. https://doi.org/10.1002/ppap.201000005
48. Liu HJ, Yang F, Zheng YM, Kang J, Qu JH, Chen JP (2011) Improvement of metal adsorption onto chitosan/Sargassum sp composite sorbent by an innovative ion-imprint technology. Water Res 45:145-154. https://doi.org/10.1016/j.watres.2010.08.017
49. Maiti N, Thomas S, Debnath A, Kapoor S (2016) Raman and XPS study on the interaction of taurine with silver nanoparticles. RSC Adv 6:56406-56411. https://doi.org/10.1039/c6ra09569k

Figures

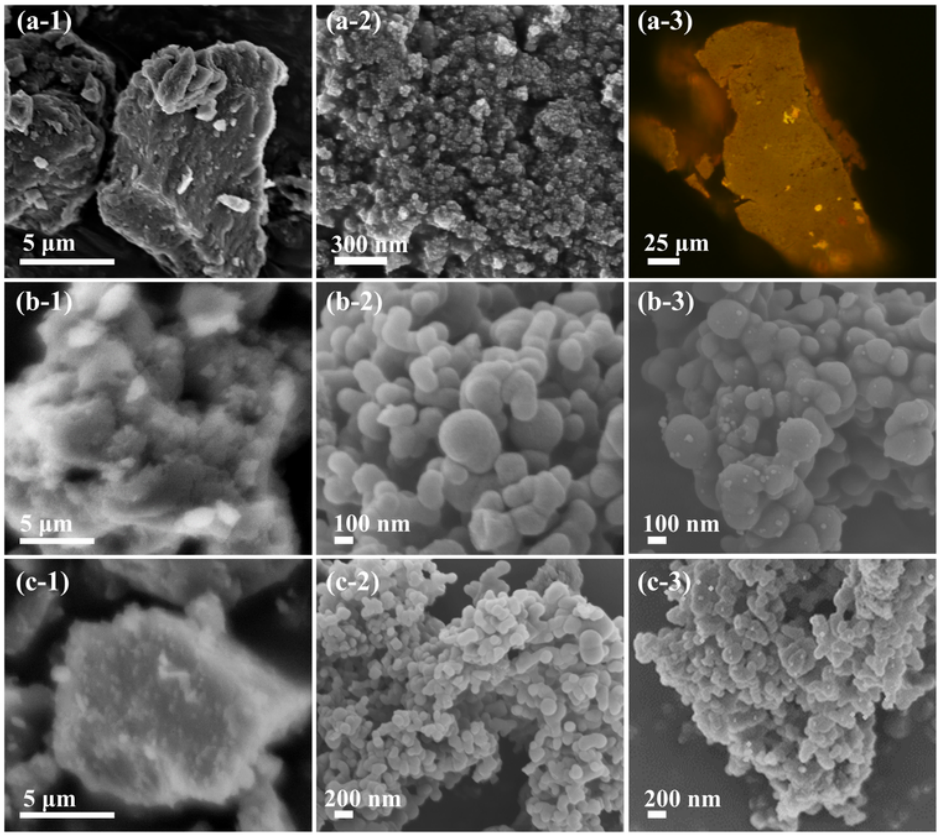

Figure 1

SEM images of (a-1) HA, (a-2) HAR, (b-1) SHA, (b-2) SHAR, (b-3) Au-SHAR, (c-1) NSHA, (c-2) NSHAR, (c-3) Au-NSHAR; fluorescence microscope image of (a-3) Au-HAR.

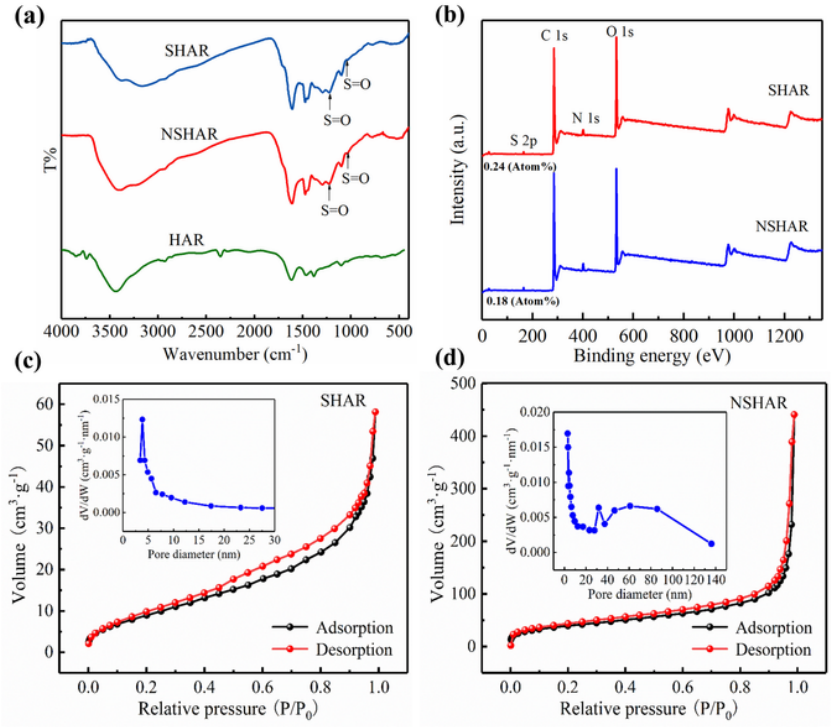

Figure 2

(a) FT-IR spectrum and (b) XPS spectra before and after sulfonated; nitrogen adsorption-desorption isotherms and corresponding pore size distributions of (c) SHAR and (d) NSHAR.

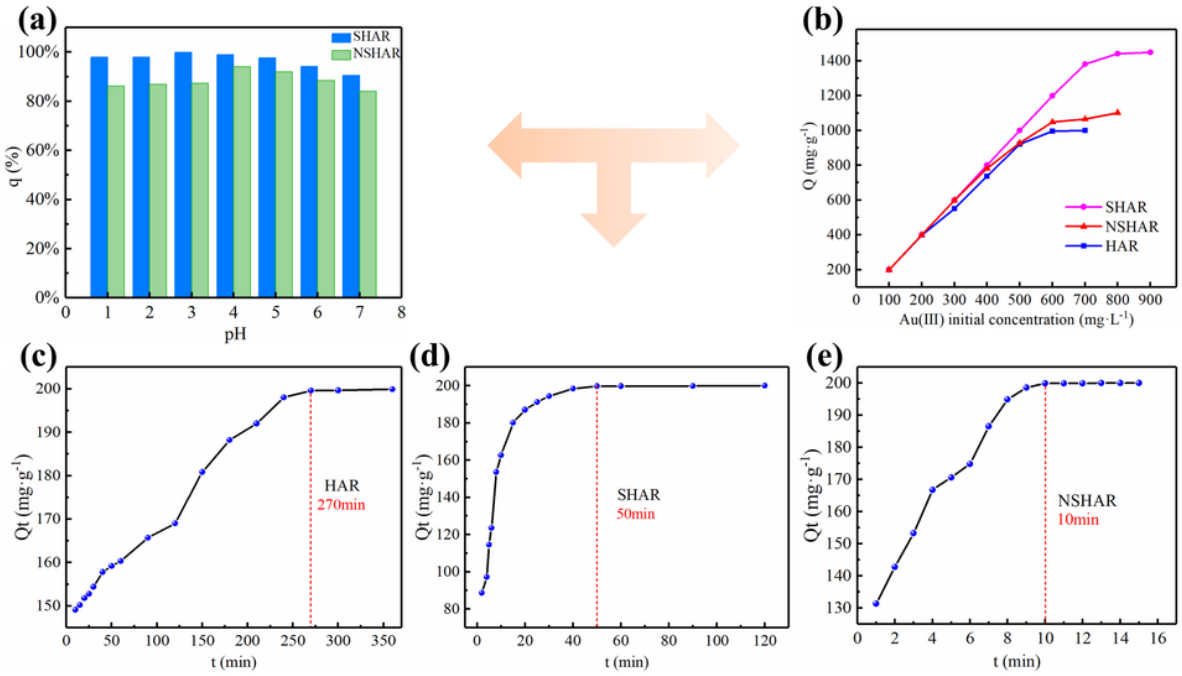

Figure 3

Adsorption capacity of Au(III) by HAR, SHAR and NSHAR at different (a) solution pH, (b) initialconcentration and (c) (d) (e)contact time.

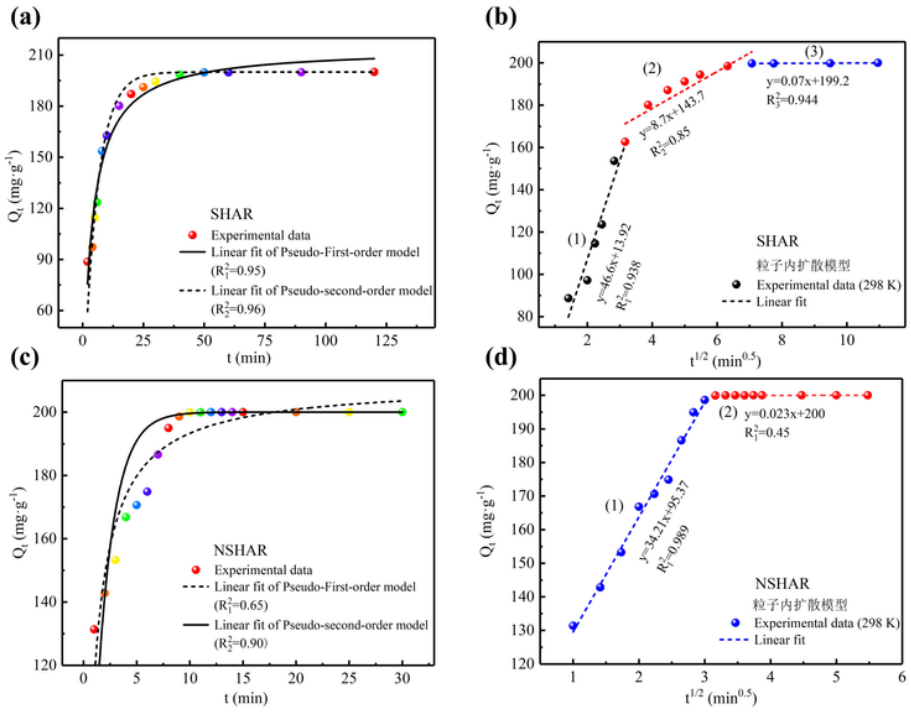

Figure 4

Models of the pseudo-first-order, pseudo-second-order and intra-particle diffusion model for Au(III) on (a) (b) SHAR and (c) (d) NSHAR. Ci=100 mg·L^{-1}, V=10 mL, m=5 mg, T=298 K.

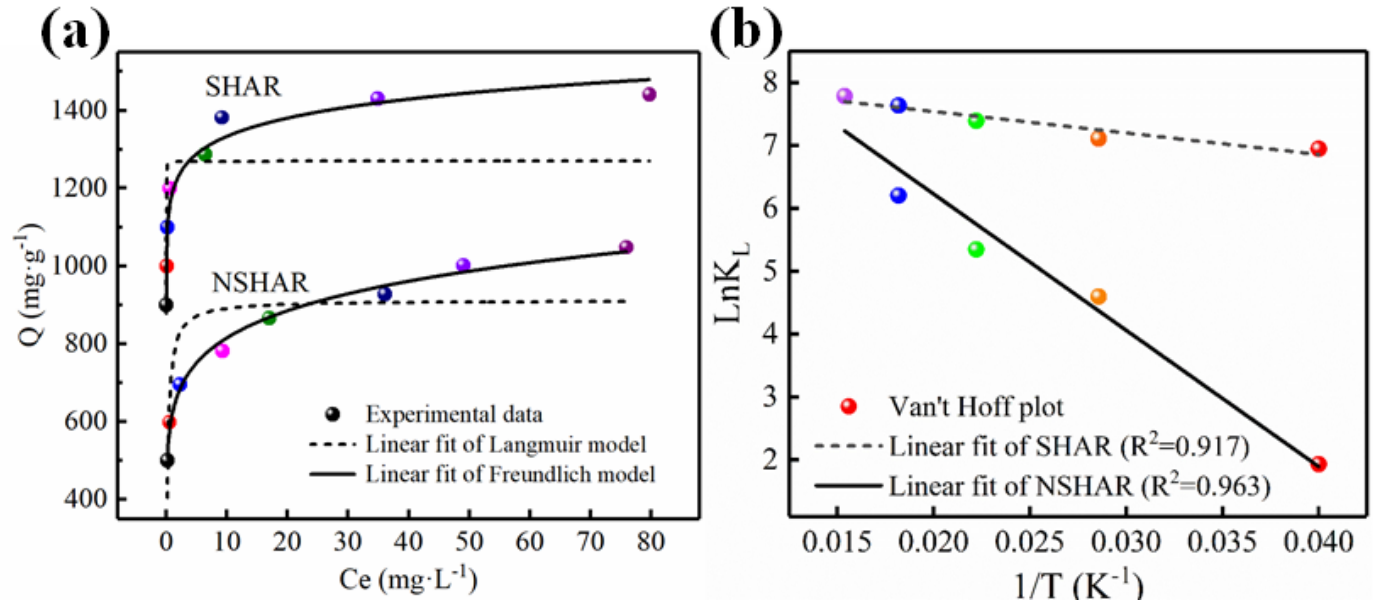

Figure 5

(a) Adsorption isotherms (298 K) and (b) Van't Hoff plot of Au(III) adsorption on SHAR and NSHAR.

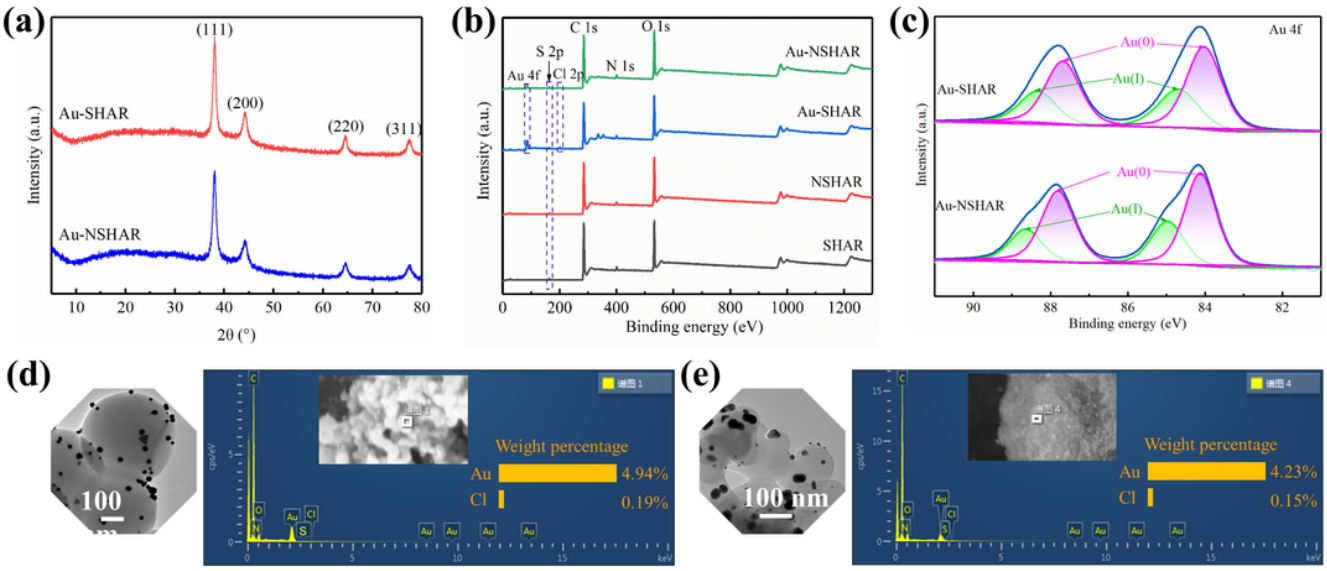

Figure 6

(a) XRD curves and (b) XPS survey spectra, (c) XPS spectra of Au 4f, TEM and SEM-EDS images of (d) Au-SHAR and (e) Au-NSHAR.

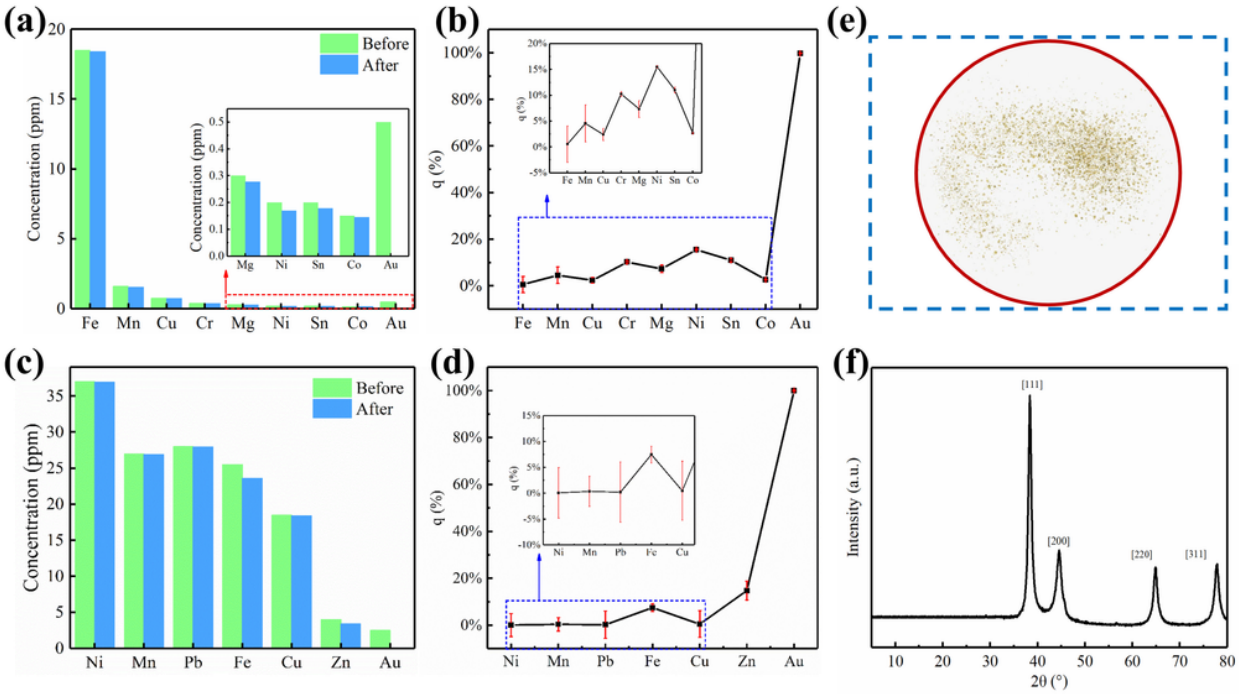

Figure 7

The concentration and adsorption ratio of competing metal ions before and after adsorption of competing metal ions in simulated (a) (b) gold ore and (c)(d) electronic board leaching solution; (e) photographs and (f) XRD spectra of Au-SHAR after calcination; (g) scheme and cost analysis of the adsorbent and gold.

Supplementary Files

This is a list of supplementary files associated with this preprint. Click to download.

- Supplementalmaterials.docx